A transmission electron microscopy study of the $(Sm,Pr)_5Co_{19}$ phase

Y. Shen and D. E. Laughlin
Department of Metallurgical Engineering and Materials Science, Carnegie Mellon University, Pittsburgh, Pennsylvania 15213

(Received 15 January 1990; accepted for publication 5 March 1990)

Transmission electron microscopy has been used to characterize the rhombohedral 5:19 phase ($R\bar{3}m$) in a stoichiometric $(Sm_{0.75}Pr_{0.25})_5Co_{19}$ alloy. In some regions, strain-induced contrast was observed in the 5:19 phase. By contrast analysis, this strain contrast was associated with a displacement vector of the type $\frac{1}{3}[01\bar{1}0]$. In other regions where the strain-induced contrast was significantly reduced, faults with the crystal structure of hexagonal $(Sm,Pr)_2Co_7$(2:7*H*) phase ($P6_3/mmc$) were observed. The formation of the faults is believed to release elastic energy within the 5:19 phase. In the interface regions between the 5:19 phase and the minor component hexagonal 2:7*H* phase, it was found by lattice imaging that the 5:19 and 2:7*H* plates are superimposed with a common c direction. The orientation relationship between the 5:19 and 2:7*H* phases is given by $[0002]_{2:7H} \| [0003]_{5:19R}$ and $[11\bar{2}0]_{2:7H} \| [11\bar{2}0]_{5:19R}$.

INTRODUCTION

The rhombohedral 5:19 phase was first discovered by Strnat and Ray in several R_5Co_{19} alloys with R = La, Ce, Pr, Nd, and Sm.[1] Like most of the intermetallic phases in rare-earth–cobalt compounds, its crystal structure can be described as a derivative of the $CaCu_5$ prototype structure (1:5), which has the space group $P6/mmm$.[1–3] The unit cell of the 5:19 structure consists of twelve 1:5 stacking units, superimposed parallel to the c axis with one Co atom replaced by a rare-earth element in every fourth layer. So far, not many microstructural studies have been conducted on any of the 5:19 phases.

The $SmCo_5$ magnet is one of the two most commonly used commercial products in high-energy permanent magnets. Efforts have been made to substitute Pr for Sm in order to increase the energy product.[4–6] In these types of $(Sm,Pr)Co_5$ modified magnets, the rhombohedral 5:19 phase is one of predominant minor components, whose presence is believed to be deleterious to the intrinsic coercivity of the magnet due to its low magnetic anisotropy field. In this study, selected-area diffraction (SAD), lattice imaging, and defect analysis are employed to characterize the $(Sm_{0.75}Pr_{0.25})_5Co_{19}$ phase.

EXPERIMENTAL CONDITIONS

A stoichiometric $(Sm_{0.75}Pr_{0.25})_5Co_{19}$ alloy was prepared using commercial-grade Pr, Sm, and Co by induction melting and was subsequently annealed at 1100 °C for 10 days. A thermomagnetic analysis (TMA) indicated that the annealed alloy consisted mainly of the 5:19 phase ($>85\%$) with a minor component of a hexagonal phase with a 2:7 phase stoichiometry and a trace amount of the 1:5 phase ($<3\%$). The specimens were prepared for examination by first dimpling the samples and then ion-milling them. Transmission electron microscopy (TEM) studies were carried out with a Phillips 420T microscope equipped with an energy dispersive x-ray spectroscopy (EDS) microanalysis detector. The microscope in the study was operated at 120 kV.

RESULTS

Consistent with the TMA study, microstructural studies by TEM indicated that the rhombohedral 5:19 phase was the dominant phase. From SAD patterns, the lattice parameters were calculated to be $a = 5.04$ Å and $c = 48.61$ Å. A distinct feature of the $(Sm_{0.75}Pr_{0.25})_5Co_{19}$ phase was the existence of strains that gave rise to a strong contrast within

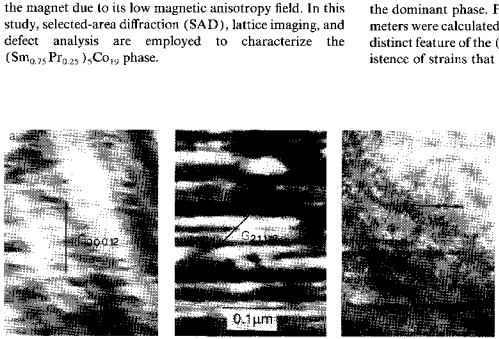

FIG. 1. Strain-induced contrast in some of the 5:19 phase regions.

 0021-8979/90/127510-04$03.00

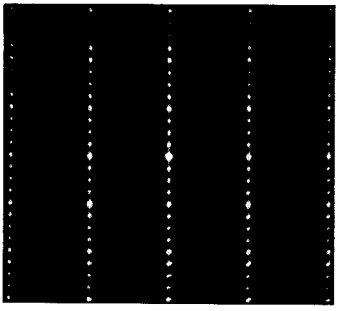

FIG. 2. Streaking was observed in the [0001] direction in strained regions of the 5:19 phase.

some of the 5:19 phase regions (Fig. 1). From trace analysis, it was found that the direction of maximum contrast was within the basal plane. In this study, hexagonal coordinates in the obverse setting are used to describe the rhombohedral phase. Since the strain contrast was minimized at $\mathbf{g} = [0\,0\,0\,12]$ and $\mathbf{g} = [2\,\bar{1}\,\bar{1}\,0]$, from a $\mathbf{g}\cdot\mathbf{R} = 0$ criterion, the strain-induced contrast originated from displacement of the type $\frac{1}{3}[01\bar{1}0]$. Streaking in the [0001] direction of the SAD pattern (Fig. 2) was observed in the heavily strained regions. Lattice imaging along the c axis (Fig. 3(a)] revealed that the 5:19 phase with the strain contrast was free of planar defects along the c axis. Because the diffraction conditions $-h + k + l = 3n$ are satisfied in the rhombohedral 5:19 phase, the spacing of the lattice image shown in Fig. 3(a) is one-third of the lattice parameter in the c direction, or 16.2 Å.

In other 5:19 phase regions of the sample, the strain-induced contrast was significantly reduced. In these regions, a large number of stacking faults were observed in the 5:19 phase (Fig. 4). The strain contrast in the presence of the faults was observed only near the faulted regions, unlike the strain contrast that occurred more uniformly in regions shown in Fig. 1. Lattice imaging of these faulted regions indicated that the crystal structure near the faults, as arrowed in Fig. 4(b), has the spacing of the hexagonal $(Sm,Pr)_2Co_7$ phase (2:7H) with a space group $P6_3/mmc$ [see and compare Fig. 3(a)]. In the unit cell of the 2:7H phase, six 1:5 stacking units are superimposed along the hexagonal c axis with substitution of a Co atom by a Pr atom in every third layer. Thus, layers 1–4 are shifted by a crystallographic shear vector $\frac{1}{3}[10\bar{1}0]$. Comparing their structures, both the 5:19 and 2:7 phases are constructed by superimposing 1:5 stacking units along the c axis with slightly different sequences of atomic substitution. The faults within the 5:19 phase with the 2:7H structure are therefore likely to occur in order to reduce the elastic strains.

The 2:7H phase is the minor component in the alloy. Based on SAD patterns of the single homogeneous 2:7H phase, the lattice parameters were calculated to be $a = 5.04$ Å and $c = 24.3$ Å. In this phase, the strain-induced contrast was not observed. Near the composition $(Sm,Pr)_2Co_7$, a rhombohedral structure with a space group $R\,\bar{3}m$ (2:7R), in which nine 1:5 stacking units are superimposed in the c direction with the replacement of a Co atom by Pr in every third layer, may also occur. Even though 2:7R and 2:7H are closely related in structure,[2,3] different reflection conditions are satisfied. In the case of the 2:7R structure with a space group $R\,\bar{3}m$, the reflection conditions are $-h + k + l = 3n$; on the other hand, 2:7H with the space group $P6_3/mmc$ obeys the reflection conditions $000l: l = 2n$; $h\,h\,\overline{2h}\,l: l = 2n$. To illustrate these reflection conditions in the closely related hexagonal and rhombohedral structures, SAD patterns of $[\bar{1}010]$ and $[\bar{2}110]$ zone axes are shown in Fig. 5 for the rhombohedral 5:19 and the hexagonal 2:7H phases, respectively. Superlattice spots along the c direction were clearly observed at one-fourth of the distance between the 1:5 fundamental spots in the SAD patterns of the 5:19 phase. The superlattice spots were observed at one-third of the distance between the 1:5 fundamental spots in the SAD patterns of the 2:7H phase. Just looking at $[\bar{1}010]$ zone patterns does not allow us to determine whether they were from a hexag-

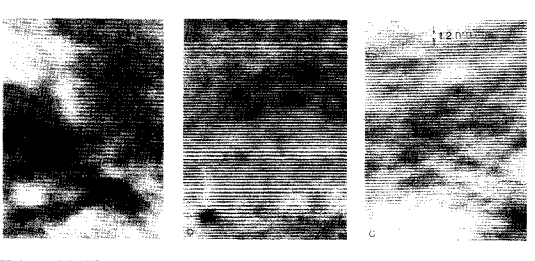

FIG. 3. Lattice images of (a) 5:19R, (b) 2:7H, and (c) the interface region of the 5:19 and 2:7H phases.

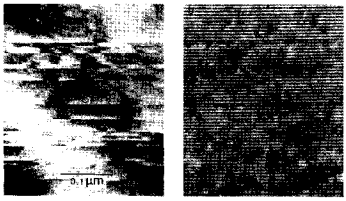

FIG. 4. The strain-induced contrast was significantly reduced when stacking faults occurred in the 5:19 matrix. Instead, the strain was observed only near the faulted regions. Arrows in lattice image indicated the regions where faults occurred.

onal phase or from a rhombohedral phase since all spots from both phases satisfied both reflection conditions. On the other hand, the information provided from extinction spots in the $[\bar{2}110]$ zone patterns was unambiguous in revealing whether the patterns were from a hexagonal phase ($P6_3/mmc$) or from a rhombohedral phase ($R\bar{3}m$). Of course, such a difference can also be revealed from [0001] SAD zone patterns. $[10\bar{1}0]$-type spots, for instance, would not appear in the [0001] zone pattern of rhobohedral phases. However, the [0001] zone pattern is almost the same as those of other binary phases in rare-earth–cobalt alloys, which are all more or less derivatives of the 1:5 prototype structure. Therefore, it is best to differentiate these phases by examining diffraction patterns in zone axes perpendicular to the c direction.

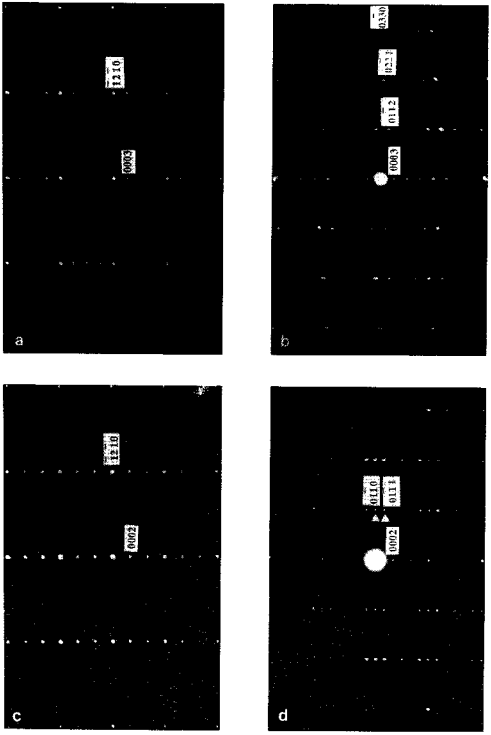

FIG. 5. (a), (b), (c), and (d) are SAD patterns of the $[10\bar{1}0]$ and $[\bar{2}110]$ zone axes for 5:19R and 2:7H phases, respectively.

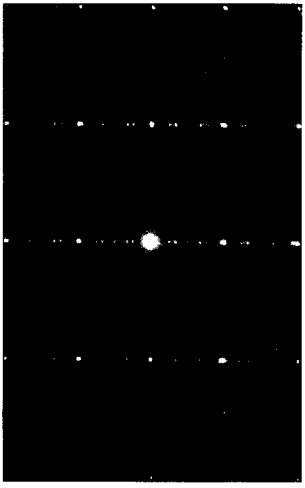

FIG. 6. The combined [$\bar{1}$010] SAD patterns of the interface region between the 2:7H and 5:19 phases, which is the superposition of Figs. 5(a) and 5(c), showed the orientation relationship between the two phases. It is given by $[0002]_{2:7H} \| [0003]_{5:19R}$ and $[11\bar{2}0]_{2:7H} \| [11\bar{2}0]_{5:19R}$.

Between the 2:7H and 5:19 phases, there was an interface region where 2:7H and 5:19 plates were superimposed along a common c axis. Lattice images of 5:19, 2:7H, and the interface regions along the c axis are shown in Fig. 3. It should be noted that the spacing in the lattice image of the 2:7H phase [Fig. 3(c)] is half of the distance of the lattice parameter c due to its reflection condition ($000l: l = 2n$). Based on the SAD pattern of the two-phase region in Fig. 6, which is the superposition of the [$\bar{1}$010] SAD patterns of 5:19 and 2:7H phases in Figs. 5(b) and 5(d), it is concluded that an orientation relationship between the two phases is given by

$$[0002]_{2:7H} \| [0003]_{5:19R}, \quad [11\bar{2}0]_{2:7H} \| [11\bar{2}0]_{5:19R}.$$

The obtained orientation relationship can be understood in terms of the structure, since both 2:7H and 5:19 phases are constructed by superimposing different numbers of approximately identical 1:5 stacking units along the c axis.

Considering the existence of a small amount of the 2:7H phase, the alloy used in our study was not exactly stoichiometric. The supersaturated 5:19 phase, within which high strains were observed (Fig. 1), was not stable and transformed to a less-strained 5:19 phase and a 2:7H phase. The phase transformation seemed to be heterogeneously in the samples. The formation of 2:7H phases within the 5:19 phase may be achieved by shearing the basal plane of the 5:19 phase in combination with short-range atomic diffusion.

ACKNOWLEDGMENTS

We wish to thank Dr. E. M. T. Velu and Professor W. E. Wallace for providing us the alloy for this study. We also would like to acknowledge useful discussions with B. K. Cheong. This work was supported by the Magnetic Materials Research Group at Carnegie Mellon University funded by National Science Foundation Grant No. DMR-86-13386.

[1] K. J. Strnat and A. E. Ray, in *Magnetism and Magnetic Materials (1974)*, edited by C. D. Graham, AIP Conf. Proc. No. 24 (American Institute of Physics, New York, 1975), p. 680.
[2] D. T. Cromer and A. C. Larson, Acta Crystallogr. **12**, 855 (1959).
[3] K. H. J. Buschow, J. Less-Common Metals **16**, 45 (1968).
[4] K. J. Strnat, IEEE Trans. Magn. **MAG-23**, 2094 (1987).
[5] M. H. Ghandeheri and J. Fidler, IEEE Trans. Magn. **MAG-21**, 1973 (1985).
[6] E. M. T. Velu, R. T. Obermyer, S. G. Sankar, and W. E. Wallace, J. Less-Common Metals **148**, 67 (1989).